Materials Letters 110 (2013) 127–129

Contents lists available at ScienceDirect

Materials Letters

journal homepage: www.elsevier.com/locate/matlet

Room temperature "one-pot" solution synthesis of nanoscale $CsSnI_3$ orthorhombic perovskite thin films and particles

Yuanyuan Zhou [a], Hector F. Garces [a], Bilge S. Senturk [a], Angel L. Ortiz [b], Nitin P. Padture [a,*]

[a] School of Engineering, Brown University, Providence, RI 02912, USA
[b] Departamento de Ingeniería Mecánica, Energética y de los Materiales, Universidad de Extremadura, 06006 Badajoz, Spain

ARTICLE INFO

Article history:
Received 19 June 2013
Accepted 1 August 2013
Available online 8 August 2013

Keywords:
Thin films
Nanoparticles
Halides
Solution synthesis

ABSTRACT

The orthorhombic perovskite polymorph of cesium tin iodide (B-γ-$CsSnI_3$) has been shown to possess an interesting combination of electrical and optical properties. Here we show that a simple "one-pot" method can be used for the solution synthesis and processing of nanoscale B-γ-$CsSnI_3$ at room temperature. This method entails the dissolution of SnI_2 and CsI powders in a specific combination of polar solvents, which results in a clear solution. Evaporation of the solvents results in the formation of B-γ-$CsSnI_3$ on substrates, either in the form of nanocrystalline thin films or nanoparticles depending on the concentration of the solution. Thus, it is not necessary to synthesize B-γ-$CsSnI_3$ phase *a priori* by vacuum melting or solid-state reaction methods before it can be solution processed, as has been implied in other studies. This has important implications for the solution synthesis and processing of nanoscale B-γ-$CsSnI_3$ phase which may find potential new uses in solid-state dye-sensitized solar cells and optoelectronic devices of the future.

1. Introduction

Cesium tin iodide, in particular the orthorhombic perovskite polymorph (B-γ-$CsSnI_3$; space group *Pnma*) [1,2] of this trihalide, is gaining rapid interest due to the possibility of its use in solid-state dye-sensitized solar cells [3–5], Schottky solar cells [6] and optoelectronic devices [2–9]. These potential applications derive from a fascinating set of room-temperature properties recently discovered in B-γ-$CsSnI_3$, which includes [2–9]: (i) high *p*-type metal-like conductivity ($\sim 200\ S\ cm^{-2}$), (ii) high hole mobility ($\sim 585\ cm^2\ V^{-1}\ s^{-1}$), (iii) direct band gap of ~ 1.3 eV, and (iv) strong near-infrared photoluminescent emission at ~ 950 nm. More recently, B-γ-$CsSnI_3$ is predicted to be a topological insulator [10]. Still, very little is known about this fascinating material, and it appears in fewer than 20 journal papers to-date.

Broadly, $CsSnI_3$ belongs to the family of perovskite trihalides $RMeX_3$ (X=halogen, Me=transition metal, and R=alkali metal or organic short chain) that are amenable to solution synthesis and processing [11]. However, synthesis and processing of B-γ-$CsSnI_3$, which is also referred to as the "black" phase, has not been explored in any detail. This is further complicated by the ready degradation of B-γ-$CsSnI_3$ in ambient air to the "yellow" Y-$CsSnI_3$ phase with a one-dimensional double-chain structure which does not possess the aforementioned desirable properties [1,2].

Scaife et al. [12], Yamada et al. [1] and Chung et al. [2,3] have synthesized B-γ-$CsSnI_3$ by melting SnI_2+CsI powder mixtures in evacuated glass vials under high vacuum, followed by slow cooling. Chung et al. [3] have shown that the melt-synthesized B-γ-$CsSnI_3$ can be completely dissolved in polar solvents. They also showed that the solution can be infiltrated into nanoporous TiO_2 for use in solid-state dye-sensitized solar cells, and inferred that the crystallized phase within the TiO_2 nanopores following evaporation of the solvent is B-γ-$CsSnI_3$ [3]. This high-vacuum melt-synthesis method has obvious drawbacks in terms of equipment needed and limitations on quantities than can be produced. Shum et al. [7] have synthesized thin films of B-γ-$CsSnI_3$ by evaporating several alternating layers of SnI_2 and CsI on a substrate, followed by heat-treating the stack to complete the solid-state reaction between the layers. This method also has the aforementioned drawbacks in terms of equipment needs and quantities produced. Furthermore, this method is limited to synthesis of thin films. Finally, Scaife et al. [12] and Shum et al. [13] have synthesized B-γ-$CsSnI_3$, in the form of powders or thin films, via direct precipitation from solutions. However, the precipitation method is not amenable to further solution processing of B-γ-$CsSnI_3$. In this context, we show here that a simple "one-pot" method can be used for the solution synthesis and processing of nanoscale B-γ-$CsSnI_3$ thin films and particles at room temperature.

2. Experimental procedure

Anhydrous CsI (Fisher Scientific, Fair Lawn, NJ) and SnI_2 (Sigma-Ardrich, St. Louis, MO) powders were obtained from commercial sources, and appropriate amounts of the two powders, 0.2054 g of CsI and 0.2946 g of SnI_2, were dissolved in 3 ml of a mixed polar

* Corresponding author. Tel.: +1 (401)863-9025; fax: +1 (401)863-2859.
E-mail address: nitin_padture@brown.edu (N.P. Padture).

0167-577X/$ - see front matter © 2013 Elsevier B.V. All rights reserved.
http://dx.doi.org/10.1016/j.matlet.2013.08.011

organic solvent. The latter consisted of a mixture of methoxyactonitrile (MOAN; Tokyo Chemical, Tokyo, Japan), dimethylformamide (DMF; Sigma-Ardrich, St. Louis, MO), and acetonitrile (AN; Fisher Scientific, Fair Lawn, NJ) in 1:3:2 volumetric proportion, respectively. The reaction was carried out for 12 h at room temperature with continuous stirring. A clear yellow solution was obtained, which showed no signs of suspended particles under Tyndall-effect laser illumination. Drops of the solution were placed on glass slides, and evaporation of the solvent was carried out under vacuum to obtain thin films of B-γ-$CsSnI_3$. Drops of ten-fold diluted solution were also placed on transmission electron microscope (TEM) sample Cu grids covered with holey carbon/graphene (EMS, Hatfield, PA), where the solvent evaporation resulted in B-γ-$CsSnI_3$ nanoparticles. All the above procedures were performed in a dry-Ar glovebox.

The thin films were characterized using room-temperature X-ray diffractometry (XRD; Bruker D8-advance, Karlsruhe, Germany) using Cu K_α radiation and the following parameters: 2θ range 10–60°, 0.02° step scan. The resulting XRD patterns were indexed with the help of the PDF2 database and analyzed quantitatively to determine the crystallite size from the peak broadening using LaB_6 as standard for correction of instrumental broadening and Voigtian line profiles [14].

The thin films were also characterized using optical microscopy, and their cross-sections (fractured) were characterized using a scanning electron microscope (SEM; LEO 1530VP, Carl Zeiss, Munich, Germany). The nanoparticles were characterized using a TEM (JEM 2100F, JEOL, Tokyo, Japan). Quantitative image analysis was used to determine the size and distribution of the nanoparticles (275 particles sample size). The TEM lattice images obtained from the nanoparticles were analyzed using Digital Micrograph software (Gatan, Pleasanton, CA).

For comparison purposes thin films were also processed using pre-reacted B-γ-$CsSnI_3$ as raw material, which was synthesized by melting in evacuated tubes. To that end, appropriate amounts of the SnI_2 and the CsI were mixed and placed in pyrex tubes. The tubes were then evacuated to 1×10^{-6} Torr vacuum for 9 h and sealed using a oxy-methane torch. The evacuated tubes were then placed in a tube furnace and heated to 550 °C (above the melting point of $CsSnI_3$ of 435 °C [2]), followed by slow cooling at a rate of 1.4 °C min^{-1} to room temperature. The tubes were opened in the glovebox, and the "black" B-γ-$CsSnI_3$ was dissolved in the above mixture of polar solvents, resulting in a clear yellow solution. Drops of the solution were place on glass slides, and evaporation of the solvent was carried out under vacuum to obtain thin films of B-γ-$CsSnI_3$.

3. Results and discussion

Fig. 1A shows indexed XRD pattern from the thin film along with an optical photo of the thin film on glass slide (inset), confirming pure B-γ-$CsSnI_3$ in the thin film, with small amount of the Cs_2SnI_6 phase present. However, the peaks are broadened, indicating nanocrystalline nature of the B-γ-$CsSnI_3$ in the thin film. Analysis of the broadening (Fig. 1B) of the strongest reflections (202 and 040) that overlap somewhat yields a crystallite size of ~33 nm. The inset in Fig. 1B shows cross-sectional SEM image of the thin film, which is ~2 μm thick.

Fig. 2A is a bright-field TEM image showing a uniform distribution of B-γ-$CsSnI_3$ nanoparticles (gray). Fig. 2B plots the measured particle size distribution of the B-γ-$CsSnI_3$ nanoparticles, resulting in an average particle size of ~26 nm. Fig. 3 is a high-resolution TEM image of B-γ-$CsSnI_3$ nanoparticle showing lattice fringes. The fringe spacing of 3.43 Å corresponds to (202) planes of B-γ-$CsSnI_3$.

Fig. 4 shows indexed XRD pattern from the thin film that was solution-processed using melt pre-reacted B-γ-$CsSnI_3$ phase.

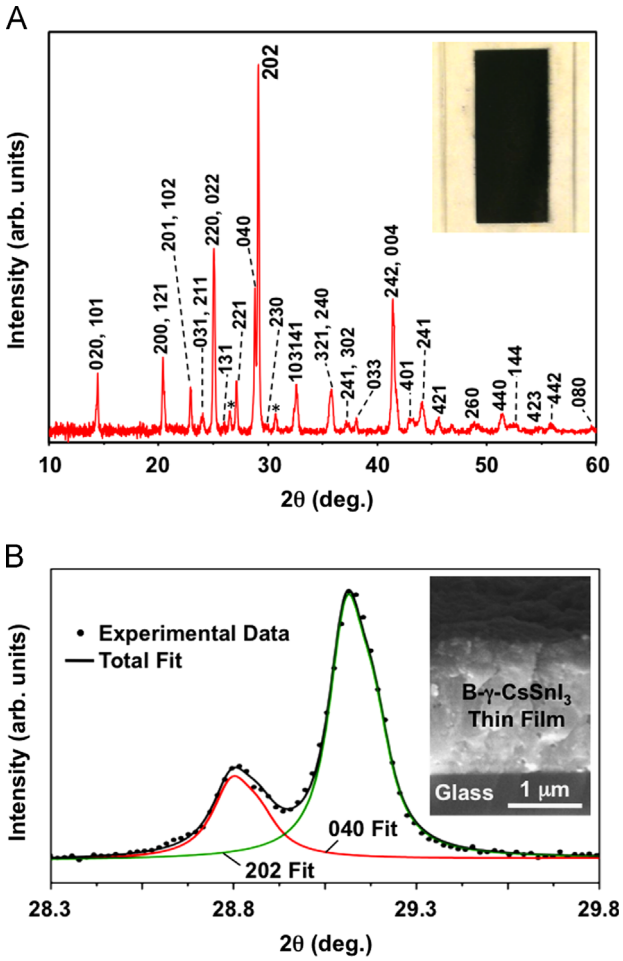

Fig. 1. XRD patterns from the thin film of B-γ-$CsSnI_3$ on glass slide solution-synthesized from CsI+SnI_2 raw materials: (A) indexed overall pattern in 2θ range 10–60°, with Cs_2SnI_6 peaks marked by '*' and (B) detailed pattern from (A) in 2θ range 28.3–29.8° showing fitting (black curve) to the XRD data (black symbols) and deconvolution of 202 (green curve) and 040 (red curve) reflections. Inset in (A) is an optical photo of the B-γ-$CsSnI_3$ thin film on a glass slide (width 25 mm). Inset in (B) is a cross-sectional (fractured) SEM image of the thin film. (For interpretation of the references to color in this figure legend, the reader is referred to the web version of this article.)

A comparison of Figs. 1A and 4 confirms that regardless of the starting raw material, mixture of CsI+SnI_2 or B-γ-$CsSnI_3$, the resulting solution-synthesized thin films are always B-γ-$CsSnI_3$ phase. Once again, small amount of the Cs_2SnI_6 phase is present. The inset in Fig. 4 is an optical photo of the B-γ-$CsSnI_3$ raw material inside an evacuated pyrex tube that was used to synthesize the thin films.

In this work we have shown that nanoscale B-γ-$CsSnI_3$ phase in the form of thin films and particles can be readily solution-synthesized using a "one-pot" approach. Furthermore, we have shown that, contrary to what has been implied [2,3], it is not necessary to synthesize B-γ-$CsSnI_3$ phase first by vacuum melting or solid-state reaction methods before it can be solution processed. While the details of B-γ-$CsSnI_3$ crystallization during evaporation are not known at this time, the reported observations can be explained using simple mechanisms. It is likely that complete dissolution of CsI and SnI_2 salts in a combination of polar organic solvents results in the dissociation reaction:

$$CsI + SnI_2 \rightarrow Cs^+ + Sn^{2+} + 3I^- \quad (1)$$

The particular composition of the polar organic solvents used in this study (MOAN:DMF:AN::1:3:2) ensures complete dissolution of the CsI and SnI_2 salts, which is key to obtaining phase-pure B-γ-$CsSnI_3$ via evaporation-crystallization. During evaporation of

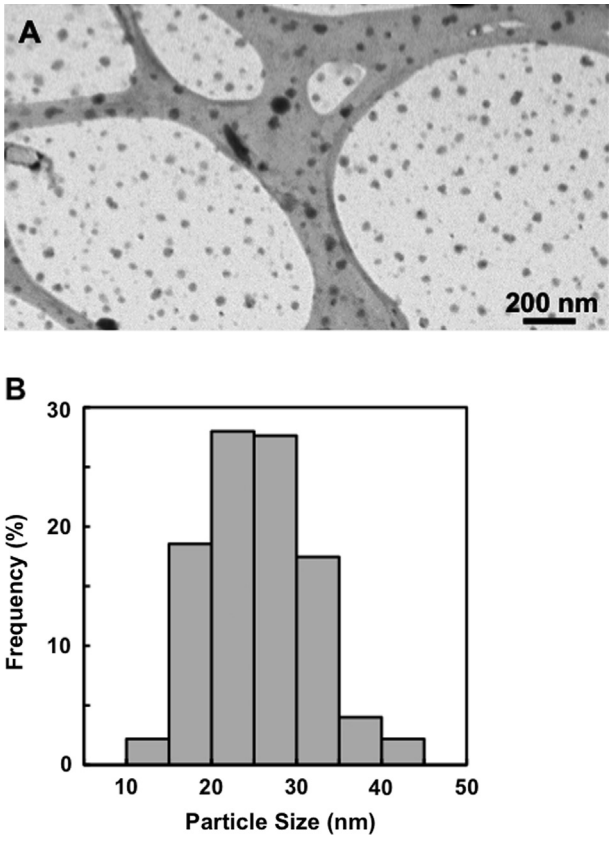

Fig. 2. (A) Bright-field TEM image of B-γ-$CsSnI_3$ nanoparticles (gray dots) synthesized on Cu TEM grids covered with holey carbon/graphene. (B) Measured B-γ-$CsSnI_3$ nanoparticles size distribution from TEM images.

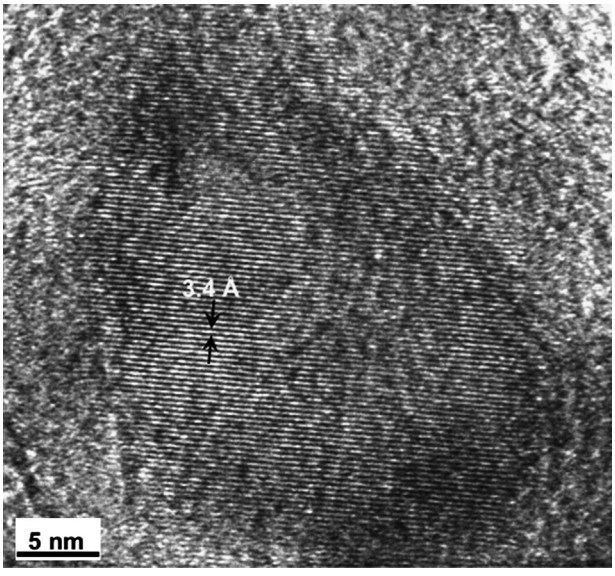

Fig. 3. High resolution TEM image of a single B-γ-$CsSnI_3$ nanoparticles showing lattice fringes corresponding to (202) planes.

the solution, B-γ-$CsSnI_3$ is the most likely phase to crystallize from Cs^++Sn^{2+}+$3I^-$ because it is the most stable phase at room temperature under dry inert gas [2]. Rapid nucleation during early stages of evaporation, followed by slow crystal growth, appears to be responsible for the nanoscale nature of the B-γ-$CsSnI_3$ synthesized in the form of thin films and particles. It is likely that complete dissociation reaction (Eq. (1)) may not occur if other polar organic solvents are used, which may be the basis for the implication by Chung et al. [2,3]

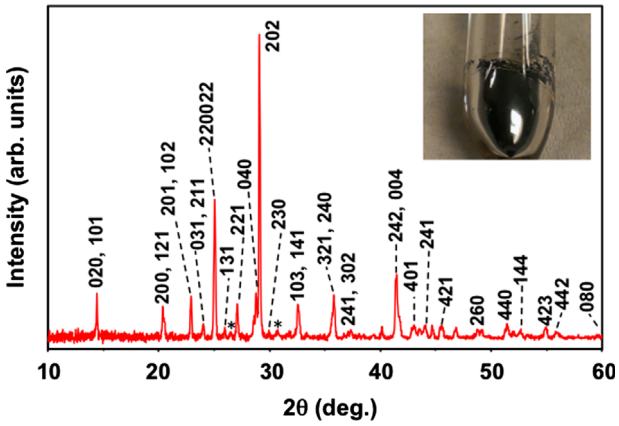

Fig. 4. Indexed XRD pattern from thin film of B-γ-$CsSnI_3$ on glass slide solution-synthesized from melt pre-reacted B-γ-$CsSnI_3$ in evacuated pyrex tube (inset; 10 mm OD), with Cs_2SnI_6 peaks marked by '∗'.

that fully-reacted B-γ-$CsSnI_3$ raw material is needed for the solution processing of B-γ-$CsSnI_3$.

4. Summary

We have demonstrated that a simple "one-pot" method can be used for the room-temperature solution synthesis and processing of nanoscale B-γ-$CsSnI_3$ in the form of thin films and particles. This method entails the dissolution of SnI_2 and CsI powders in a specific mixture of polar solvents, followed by the evaporation of the solvent. Thus, it is not necessary to synthesize B-γ-$CsSnI_3$ phase *a priori* by vacuum melting or solid-state reaction methods before it can be solution processed, as implied in other studies. This has important implications for the solution synthesis and processing of nanoscale B-γ-$CsSnI_3$ phase that is showing very interesting properties, and which is finding potential new uses in solid-state dye-sensitized solar cells and optoelectronic devices of the future.

Acknowledgment

The authors are grateful for the partial support from NSF under Grant no. DMR-1305913, and thank Prof. G. Diebold for assistance with evacuated pyrex tubes.

References

[1] Yamada K, Funabiki S, Horimoto H, Matsui T, Okuda T, Ichiba S. Chemical Letters 1991;5:801–4.
[2] Chung I, Song J-H, Im J, Androulakis J, Malliakas CD, Li H, et al. Journal of the American Chemical Society 2012;134:8579–87.
[3] Chung I, Lee B, He J, Chang RPH, Kanatzidis M. Nature 2012;485:486–90.
[4] Mallouk TE. Nature 2012;485:450–1.
[5] Bach U, Daeneke T. Angewandte Chemie International Edition 2012;51:10451–2.
[6] Chen Z, Wang JJ, Ren Y, Yu C, Shum K. Applied Physics Letters 2012;101:093901.
[7] Shum K, Chen Z, Qureshi J, Yu C, Wang JJ, Pfenninger W, et al. Applied Physics Letters 2010;96:221903.
[8] Yu C, Chen X, Wang JJ, Pfenninger W, Vockic N, Kenney JT, et al. Journal of Applied Physics 2011:110.
[9] Chen Z, Yu C, Shum K, Wang JJ, Pfenninger W, Vockic N, et al. Journal of Luminescence 2012;132:345–9.
[10] Jin H, Im J, Freeman AJ. Physical Review B 2012;86:121102(R).
[11] Mitzi DB. Synthesis, structure, and properties of organic-inorganic perovskites and related materials. In: Karlin KD, editor. Progress in Inorganic Chemistry. New York: John Wiley & Sons; 1999. p. 5–45.
[12] Scaife DE, Weller PF, Fisher WG. Journal of Solid State Chemistry 1974;9:308–14.
[13] Shum K, Chen Z, Ren Y. United States Patent Application No. 0306053 A1; 2012.
[14] Sanchez-Bajo F, Ortiz AL, Cumbrera FL. Journal of Applied Crystallography 2006;39:598–600.